Gene Expression Profile of Human Airway Epithelium Induced by Hyperoxia *In Vivo*

Arnaud Chambellan, Paul J. Cruickshank, Patrick McKenzie, Steven B. Cannady, Katalin Szabo, Suzy A. A. Comhair, and Serpil C. Erzurum

Institut du Thorax, INSERM U533, Faculté de Médecine, Nantes, France; and Departments of Pathobiology, Pulmonary, Allergy, and Critical Care Medicine, The Head and Neck Institute, The Cleveland Clinic Foundation, Cleveland, Ohio

Hyperoxia leads to oxidative modification and damage of macromolecules in the respiratory tract with loss of biological functions. Given the lack of antioxidant gene induction with acute exposure to 100% oxygen, we hypothesized that clearance pathways for oxidatively modified proteins may be induced and serve in the immediate cellular response to preserve the epithelial layer. To test this, airway epithelial cells were obtained from individuals under ambient oxygen conditions and after breathing 100% oxygen for 12 h. Gene expression profiling identified induction of genes in the chaperone and proteasome-ubiquitin-conjugation pathways that together comprise an integrated cellular response to manage and degrade damaged proteins. Analyses also revealed gene expression changes associated with oxidoreductase function, cell cycle regulation, and ATP synthesis. Increased HSP70, protein ubiquitination, and intracellular ATP were validated in cells exposed to hyperoxia *in vitro*. Inhibition of proteasomal degradation revealed the importance of accelerated protein catabolism for energy production of cells exposed to hyperoxia. Thus, the human airway early response to hyperoxia relies predominantly upon induction of cytoprotective chaperones and the ubiquitin-proteasome–dependent protein degradation system to maintain airway homeostatic integrity.

Keywords: airways; gene expression; hyperoxia; proteasome; ubiquitin

Oxygen, one of the most abundant elements in our world, is essential for the oxidation of organic compounds to generate the energy needed to sustain life. Under ambient conditions, reactive oxygen species (ROS) are generated at a low level in lung cells during aerobic metabolism. To minimize the oxidant injury that is a consequence of aerobic life, the human lung is endowed with an integrated antioxidant system, which detoxifies reactive products (1–4). However, excessive ROS may overwhelm the antioxidant system and result in damage to major cellular components, including membrane lipids, proteins, carbohydrates, and DNA (1, 5–8). The pathophysiologic consequences of this injury may include cell death, and tissue inflammation and damage. This is particularly evident during conditions of increased oxygen exposure for medical therapy (4, 9, 10). The bronchial epithelium is particularly vulnerable to the effects of airborne oxidative stress as the moist mucosal surface of the airway is in direct contact with the environment (11). Hyperoxia leads to oxidant injury in the respiratory tract, which is manifest as acute tracheobronchitis with edema and decrease in mucociliary clearance (12, 13). Oxidative damage of proteins and loss of biological function is one defined end-point of hyperoxic injury (1, 5–8). In the past, significant attention has focused on clarifying the role of antioxidant enzymes such as superoxide dismutases, catalase, or glutathione peroxidases in mitigating airway damage resulting from hyperoxia (6, 7, 12, 14, 15). Studies show that exposure to lower levels of hyperoxia can lead to upregulation of antioxidant defenses, which are protective in subsequent high-level ($> 95\%$) oxygen exposure (1). However, most studies also show that in response to immediate exposure to $> 95\%$ oxygen, antioxidant enzymes are expressed at low levels, and are unable to upregulate rapidly enough to protect against injury (6, 7, 12, 15). In this context, we hypothesized that in the absence of increased protection against oxidative injury, clearance pathways for oxidatively damaged proteins may have a central role in the early response of cells to maintain the homeostatic integrity of the epithelial layer. Substantial evidence indicates that the ubiquitin-proteasome system is responsible for degrading altered proteins in the cytoplasm, nucleus, and endoplasmic reticulum of eukaryotic cells (16). Using a functional genomic approach, we analyzed the mRNA levels of human bronchial epithelial cells obtained by brushing at bronchoscopy from healthy volunteers before and after 12 h exposure to $> 95\%$ oxygen. Genes related to proteasome ubiquitin-dependent protein catabolism, cell cycle, or with an oxidoreductase activity were identified as primary early responses to *in vivo* hyperoxia. In complementary studies, the induction of chaperones, ATP synthesis, and increased ubiquitination was confirmed in human airway epithelial cells exposed to hyperoxia *in vitro*.

MATERIALS AND METHODS

Study Population and Exposure to Hyperoxia *In Vivo*

To evaluate human bronchial epithelial cell hyperoxia-related gene expression *in vivo*, healthy nonsmoking volunteers were studied. All had normal histories, physical examinations, chest X-ray, and spirometry. Exclusion criteria included prolonged exposure to second-hand smoke at home or work; exposure to environmental dusts or toxic agents known to cause pulmonary disease; a history of recurrent episodes of breathlessness, chest tightness, cough, and/or sputum production; human immunodeficiency virus infection; and a history of respiratory infection in the previous 6 wk (7, 12). Volunteers underwent fiberoptic bronchoscopy with cytology brushings from the right main stem bronchus to obtain bronchial epithelial cells at room air (group normoxia). They returned 2 wk later and were exposed at $> 95\%$ oxygen for 12 h by a full, tight-fitting mask, after which they immediately underwent a bronchoscopy for sampling of bronchial epithelial cells (group hyperoxia) as previously described (7, 12, 17). In addition, other healthy volunteers underwent bronchoscopy to collect bronchial epithelial cells for culture with exposure to normoxia and hyperoxia *in vitro*. The study was approved by the Institutional Review Board, and written informed consent was obtained from all volunteers.

Preparation of RNA and Microarray Hybridization

Normal bronchial epithelial cells were obtained by cytology brushings from second- and third-order bronchi as previously described (12).

(*Received in original form July 8, 2005 and in final form May 4, 2006*)

This study was supported by AI70649, HL60917, and M01 RR018390 from the National Center for Research Resources. A.C. was supported by grants from the Collège des Professeurs de Pneumologie.

Correspondence and requests for reprints should be addressed to Serpil C. Erzurum, M.D., Chair, Department of Pathobiology, Cleveland Clinic Foundation, Lerner Research Institute, 9500 Euclid Ave/NC22, Cleveland, OH 44195. E-mail: erzurus@ccf.org

Am J Respir Cell Mol Biol Vol 35. pp 424–435, 2006
Originally Published in Press as DOI: 10.1165/rcmb.2005-0251OC on May 11, 2006
Internet address: www.atsjournals.org

Total RNA from fresh human bronchial epithelial cells was isolated by the Guanidium Thiocyanate-Cesium Chloride (GTC-CsCl) gradient method, and first subjected to formaldehyde-agarose gel electrophoresis to confirm its integrity. Samples showing degradation of ribosomal RNA by visual inspection under ultraviolet light were discarded. Total RNA (8 μg) was converted into double-stranded cDNA with the SuperScript II reverse transcriptase (Invitrogen, Carlsbad, CA) using an oligo$(18)_{24}$ primer containing a T7 RNA polymerase promoter (Genset, La Jolla, CA). cDNAs were purified by phenol/chloroform extraction and ethanol precipitation. The cDNA was used as a template for synthesis of the biotinylated cRNA transcript using the BioArray RNA transcript labeling kit (Enzo Diagnostics, Farmingdale, NY). cRNAs were purified from an *in vitro* transcription reaction using RNeasy kit (Qiagen, Valencia, CA). After fragmentation into ≈ 200 bp by alkaline treatment (200 mM tris-acetate, pH 8.2/500 mM potassium acetate/150 mM magnesium acetate), biotinylated cRNA was hybridized to the test chip as specified by Affymetrix; when satisfactory, 15μg of the labeled cRNA were hybridized overnight onto the Affymetrix HG-U133A GeneChip (Affymetrix, Santa Clara, CA), which contained 22,283 human transcripts. After hybridization, each array was washed and stained according to the Affymetrix protocol EukGE-WS2v4, and scanned (GeneArray scanner G2500A; Hewlett-Packard, Palo Alto, CA). The methodology used in our study fulfilled the Microarray Gene Expression Data Society (MGED) Minimum Information About a Microarray Experiment (MIAME) guidelines (www.mged.org/Workgroups/MIAME/miame.html).

Microarray Data Acquisition and Preprocessing

From data image files, gene transcript levels were determined using algorithms from the Microarray Analysis Suite version 5.1 software (Affymetrix). Based on the detected *P* value, a single weighted mean expression level for each gene was obtained, as well as the absolute call (designated "Present," "Marginal," or "Absent"), indicating if the transcript was reliably detected using a one-sided Wilcoxon signed-rank test. Data was scaled from each array to normalize the results for interarray comparisons by correcting the mean intensity for each array (top and bottom 2% of genes excluded) to a set target intensity of 300. Arrays were assessed for several quality control measures, including the absence of any significant artifacts, the detection *P* value < 0.05 (called "Present") for the bacterial genes spiked into the hybridization mix, the 3′/5′ ratio of the intensity for β-actin and GADPH, the percent of genes detected as "Present" in each array. Finally, probe sets designated as "Absent" were filtered out in all arrays.

Microarray Data Analysis

The raw data, normalized using the GeneSpring software (Silicon Genetics, Redwood City, CA), was performed as follows: (*1*) per microarray sample, by dividing the raw data by the 50th percentile of all measurements; and (*2*) per gene, by dividing the raw data by the median of the expression level for the gene in all samples. All further analyses were performed on the 9,787 normalized genes from 8 chips. The gene annotations for each probe set were updated with the latest NetAffx HG-U133A annotation file (09–16–2005) at: http://www.affymetrix.com/support/technical/byproduct.affx?product=hgu133-20 (19). Assessment of genes with significant change was performed using the GeneSpring software, by calculating the *P* values using the Welch *t* test. This analysis was done on the 9,787 genes from 8 chips. Genes were assumed to be significantly upregulated or downregulated if the calculated *P* value was < 0.05. The mean value of expression for a given gene in hyperoxia and normoxia was used to determine the fold change in a gene expression between the two conditions. Hierarchical clustering of the genes among samples from individuals in normoxia and in hyperoxia was performed by a Pearson correlation (uncentered) similarity metric and average linkage clustering using the GeneSpring software tools applying Eisen's methodology (20). Selected genes were subjected to an intensive search to identify biological function and associated regulatory pathways. Genes were classified based on the Gene Ontology Consortium (21) obtained through the NetAffx server (available at www.netaffx.com), public information from GenBank (www.ncbi.nlm.nih.gov/Genbank/index.html), and SOURCE search (http://genome-www5.stanford.edu/cgi-bin/source/sourceSearch) for biological process. To identify functional categories that were modulated by hyperoxia, we used the GOMINER software developed by Zeeberg and coworkers, which gives a *P* value for Gene Ontology (GO) categories that are enriched in significantly modulated genes (22).

Cell Culture and *In Vitro* Hyperoxia

BET-1A cells, a human bronchial epithelial cell line transformed by SV-40 T antigen (23), was cultured in a serum-free LHC-9 medium consisting of LHC-8 medium (Biofluids, Rockville, MD), 2.75 M epinephrine, 0.33 nM retinoic acid, 25 U/ml penicillin, 25 μg/ml streptomycin, and 25 μg/ml fungizone (Invitrogen), on plates precoated with coating medium containing 29 μg/ml collagen (Vitrogen, Palo Alto, CA), 10 μg/ml bovine serum albumin (Biofluids, Camarillo, CA), and 10 μg/ml fibronectin (Calbiochem, La Jolla, CA). Primary human airway epithelial cells (HAEC) obtained by bronchial brushing from healthy volunteers were cultured in serum-free Lechner and LaVeck media (LHC8) on plates precoated with coating media as above (24). Primary HAEC cultures of passages 0–2 were used in experiments. HAEC or BET-1A were placed in a humidified incubator chamber (MIC-101; Billups-Rothenburg, Del Mar, CA), and the chamber inlet port connected to a source of pure oxygen infused at 5 liters/min. Oxygen concentration was monitored at the outlet port, and when oxygen was $> 98\%$ in the chamber, the gas source was disconnected and inlet and outlet ports tightly clamped. The chamber was maintained in an incubator at 37°C for the duration of the exposure, and the oxygen monitored at the end of the exposure. At end of exposures of up to 24 h oxygen levels were $98 \pm 2\%$. After exposure, the cells were rinsed three times with phosphate-buffered saline and harvested for RNA and protein extracts.

To evaluate the effect of hyperoxia on ubiquitination of proteins, 50 μM proteasome inhibitor Ac-Leu-Leu-nLeu-al (ALLN; Santa Cruz Biotechnology, Santa Cruz, CA) was added before hyperoxia to block proteasome degradation.

Northern Blot Analysis

Total RNA from cells was extracted by the GTC ([4 M guanidium thiocyanate, 25 mM sodium citrate, pH 7.0], 0.5% sarkosyl, and 0.1 M β–mercaptoethanol)-CsCl gradient method and evaluated by Northern blot using a [^{32}P]-labeled Heat Shock Protein 70 (HSP70) probe (25, 26) and [^{32}P]-labeled 18S ribosomal RNA as a control. The blots were then subjected to autoradiography and the HSP70 bands quantified relative to 18S ribosomal RNA using a PhosphorImager (Molecular Dynamics, Sunnyvale, CA).

Western Blot Analysis

BET-1A cells were harvested in an ice-cold buffer containing 50 mM Tris (pH 7.9), 50 mM NaCl, 1 mM EDTA, 1 mM dithiothreitol (DTT), 0.5% Nonidet P-40, 10% glycerol, 1 mM phenylmethylsulphonylfluoride (PMSF), 5 μg/ml leupeptin, 10 μg/ml pepstatin A, 200 μM sodium orthovanadate (NaOV), and 20 μg/ml aprotinin (24, 27). Cell lysates (70 μg/lane) were separated by electrophoresis on 15% SDS-PAGE HCl gel and then electrophoretically transfered onto a nitocellulose membrane or onto Immuno-Blot PVDF Membrane (0.2 μm; Bio-Rad, Hercules, CA). The membrane was blocked with 5% nonfat milk or 5% bovine serum albumin (BSA; Biosource, Rockville, MD), and incubated overnight with primary antibodies. Antibodies included monoclonal anti-ubiquitin antibody P4D1 (Santa Cruz Biotechnology), the rabbit polyclonal cleaved caspase-8 antibody (Cell Signaling Technology, Danvers, MA), the mouse monoclonal anti–β-actin antibody AC-15 (Sigma-Aldrich, St. Louis, MO), and the secondary antibody was conjugated to horseradish peroxidase. The detection of signal was performed with enhanced chemiluminescent system (ECL; Amersham, Arlington Heights, IL).

Measurement of Intracellular ATP Concentration

Whole cell protein extracts from BET-1A cells were harvested as described above. ATP concentration within lysates was detected using the ATPlite Luminescence ATP Detection Assay System (PerkinElmer, Boston, MA). Values were normalized for protein concentrations of the lysate.

RESULTS

Clinical Assessment of Healthy Volunteers and Biological Samples

Global characteristics of healthy volunteers included average age of 27 ± 2 yr, 3 females, and all were white. The major epithelial cell types obtained by brushing at bronchoscopy included ciliated, secretory, basal, and undifferentiated cells, and a small number of inflammatory cells as previously reported (7). A total of six individuals were analyzed by microarray. Two chips, representing paired RNA from one volunteer under normoxia and hyperoxia, displayed a poor microarray quality score and were not used in analyses. Of the remaining five individuals, RNA was degraded in one of the five under normoxia, and in another one of five under hyperoxia. Thus eight chips representing five individuals, with three of the five individuals having paired data before and after hyperoxia, were of good quality and used in analyses (Table 1).

Global Analysis of Gene Expression Profiles

Based on the selection of genes called "Present," and those found in at least three of four chips in each condition (normoxia or hyperoxia), a total of 9,787 genes were identified in the final set of analyzed genes. Based on the Welch *t* test, we identified 135 genes (1.4% of the total genes) significantly modulated by hyperoxia—that is, 97 up-regulated genes and 38 down-regulated genes (Tables 2 and 3). Fold change of modulated genes was modest: 6% of these genes displayed on average ± 60% variation in hyperoxia versus normoxia, 19% displayed ± 40–60% variation, 58% displayed ± 20–40% variation, and 17% of the genes had < 20% variation. Consequently, the *P* value for each gene from the Welch *t* test was obtained without any correction for false discovery rate (Figure 1). The effects of hyperoxia were also assessed through the complementary approach of global analysis of gene expression by the clustering method. This approach identified individuals rather than the hyperoxia exposure within the whole set of 9,787 genes (Figure 2A). Hyperoxia exposure was discriminated by gene expression profile when the subgroup of genes for analyses was selected upon the *P* value < 0.05 (i.e., the set of 135 significantly modulated genes; Figure 2B). To mitigate any difficulty with false detection, we focused on the functional categories according to the Gene Ontology (GO) denomination rather than on the modulation of specific genes by themselves. Functional analysis was extrapolated through the GO categories for each gene, with the aid of the GOMINER software (22) (Table 4). This approach identified the involvement of several groups of genes with particular known molecular functions and biological processes and thus helps the understanding of the complex integrated hyperoxia-induced cell response (Figures 3A and 3B). Categories of genes involved in protein modification were predominantly identified, especially genes with oxidoreductase activity and those involved in ubiquitination. There was also induction of genes involved in ATP synthesis. Of note, a group of genes with unknown function was also identified. Some of these, however, belong to well-defined categories such as the ubiquitin-dependent protein catabolism for PSMD9 or protein ser/thr/tyr kinase activity for LIMK2; the grouping shown is inherent to the GO classification.

Selected Pathways and Categories of Interest from the Functional Analysis

Antioxidants, redox-related genes, and glutathione metabolism. Antioxidant enzymes including the superoxide dismutases (SOD), catalase, glutamylcysteine ligase (GCL), or glutathione peroxidases (GPx) were not significantly modulated by hyperoxia (Table 5). The functional analysis identified genes with oxidoreductase activity instead (Table 4). This group includes alcohol dehydrogenases especially involved in the metabolism of lipid peroxidation products, suggesting a pivotal role of redox homeostasis in hyperoxia response. The glutathione metabolism category was not identified by functional analyses. However, genes related to glutathione/thiol metabolism were significantly modulated in the gene expression analysis, such as glutaredoxin 2 (GLRX2) and alcohol dehydrogenase 5 (ADH5). GLRX2 catalyzes the glutathione-dependent reduction of disulfides and glutathione-mixed disulfides in the mitochondrion (18, 28), whereas ADH5, a ubiquitous protein widely distributed in mammals, acts as a glutathione-dependent formaldehyde dehydrogenase, controlling intracellular levels of S-nitrosoglutathione, S-nitrosylated proteins, and the metabolism of lipid peroxidation products (29, 30). Together these enzymes contribute to cellular redox homeostasis.

Ubiquitination and protein catabolism pathway. The ubiquitin-dependent protein catabolism and protein modification categories were the foremost biological process identified by the functional analysis using the GOMINER approach (Table 4, Figure 3). Among the genes identified in this category were proteasome subunit α1 (PSMA1), ubiquitin-conjugating enzyme E2E1 (UBE2E1), ubiquitin-conjugating enzyme E2L3 (UBE2L3), ubiquitin-specific protease 24 (USP24), and PSMD9 (Table 3).

Genes involved in the response to stress and inflammation. Chaperones from the heat shock 70-kD (HSP70) and 40-kD (HSP40) family were induced by hyperoxia; that is, heat shock 70-kD protein 5-glucose-regulated protein (HSPA5), which is the only heat shock from the endoplasmic reticulum in the set of 9,784 genes, and DnaJ (HSP40) homolog subfamily B member

TABLE 1. EVALUATION OF THE QUALITY FILTER CRITERIA IN MICROARRAY CHIPS

Name	Background < 100	Noise < 5	Scale Factor*	%P†	3′/5′ β-actin < 2	3′/5′ GAPDH < 2
1-normoxia	59	2.5	13.4	42	2.5	1.6
2-normoxia	89	3.8	4.4	52	1.2	0.9
2-hyperoxia	80	3.3	4.2	54	1.3	1.1
3-normoxia	100	4.2	6.1	46	1.4	1,0
3-hyperoxia	93	3.9	3.6	54	1.2	1,0
4-normoxia	70	3.1	6.1	53	1.0	0.9
4-hyperoxia	84	3.5	10.6	46	1.2	0.8
5-hyperoxia	81	3.6	8.2	50	1.4	0.9
Mean (70)	82 (13)	3.5 (0.5)	7.1 (3.4)	50 (4)	1.4 (0.5)	1 (0.2)

Definition of abbreviation: GAPDH, glyceraldehyde phosphate deydrogenase.

* Scaling factor of the mean intensity for each array to a set target intensity of 300.

† Percent of genes detected as Present by the Microarray Suite 5.1 software.

TABLE 2. GENES DOWN-REGULATED IN AIRWAY EPITHELIUM WITH HYPEROXIA *IN VIVO*

Affymetrix ID	Accession No.	Symbol	Gene	Ratio*	*P* Value†
221904_at	NM_144635	MGC21688	Hypothetical protein MGC21688	0.73	2.5×10^{-3}
219001_s_at	NM_024345	MGC10765	Hypothetical protein MGC10765	0.66	3.4×10^{-3}
221774_x_at	NM_017569	FAM48A	Family with sequence similarity 48, member A	0.64	3.7×10^{-3}
32091_at	NM_014655	KIAA0446	KIAA0446 gene product	0.81	7.2×10^{-3}
204676_at	NM_015421	DKFZP564K2062	DKFZP564K2062 protein	0.67	1.2×10^{-2}
204252_at	NM_001798	CDK2	Cyclin-dependent kinase 2	0.72	1.3×10^{-2}
212083_at	NM_144582	TEX261	Testis expressed gene 261	0.85	1.3×10^{-2}
200856_x_at	NM_006311	NCOR1	Nuclear receptor co-repressor 1	0.61	1.6×10^{-2}
204180_s_at	NM_014007	ZNF297B	Zinc finger protein 297B	0.80	1.7×10^{-2}
206115_at	NM_004430	EGR3	Early growth response 3	0.40	1.8×10^{-2}
213816_s_at	NM_000245	MET	Met proto-oncogene (hepatocyte growth factor receptor)	0.67	1.9×10^{-2}
201860_s_at	NM_000930	PLAT	Plasminogen activator, tissue	0.64	1.9×10^{-2}
219801_at	NM_030580	ZNF34	Zinc finger protein 34 (KOX 32)	0.69	2.1×10^{-2}
215246_at	NM_016648	HDCMA18P	HDCMA18P protein	0.77	2.3×10^{-2}
203934_at	NM_002253	KDR	Kinase insert domain receptor (a type III receptor tyrosine kinase)	0.75	2.5×10^{-2}
201668_x_at	NM_002356	MARCKS	Myristoylated alanine-rich protein kinase C substrate	0.83	2.7×10^{-2}
37433_at	NM_004671	PIAS2	Protein inhibitor of activated STAT2	0.64	2.7×10^{-2}
201270_x_at	NM_015332	KIAA1068	KIAA1068 protein	0.84	2.8×10^{-2}
206533_at	NM_000745	CHRNA5	Cholinergic receptor, nicotinic, α polypeptide 5	0.72	2.9×10^{-2}
214801_at	NM_145034	LOC163590	AF464140	0.66	3.0×10^{-2}
216396_s_at	NM_004879	EI24	Etoposide induced 2.4 mRNA	0.78	3.0×10^{-2}
209594_x_at	NM_002784	PSG9	Pregnancy-specific β1-glycoprotein 9	0.78	3.0×10^{-2}
217156_at	NM_000182	HADHA	Hydroxyacyl-Coenzyme A dehydrogenase/3-ketoacyl-Coenzyme A thiolase/enoyl-Coenzyme A hydratase (trifunctional protein), α subunit	0.66	3.1×10^{-2}
219685_at	NM_021637	FLJ14084	Hypothetical protein FLJ14084	0.73	3.2×10^{-2}
210653_s_at	NM_000056	BCKDHB	Branched chain keto acid dehydrogenase E1, β polypeptide (maple syrup urine disease)	0.79	3.2×10^{-2}
217866_at	NM_024811	FLJ12529	Pre-mRNA cleavage factor I, 59-kD subunit	0.86	3.5×10^{-2}
213058_at	AK092338	LOC283585	Transcribed locus, weakly similar to XP_375099.1 hypothetical protein LOC283585	0.63	3.6×10^{-2}
214699_x_at	NM_015610	DKFZP434J154	WIPI49-like protein 2	0.72	3.6×10^{-2}
217682_at	NM_014117	PRO0149	PRO0149 protein	0.80	3.6×10^{-2}
205741_s_at	NM_001392	DTNA	Dystrobrevin, α	0.72	3.9×10^{-2}
218862_at	NM_024701	ASB13	Ankyrin repeat and SOCS box-containing 13	0.82	4.1×10^{-2}
214119_s_at	NM_000801	FKBP1A	FK506 binding protein 1A, 12 kD	0.68	4.1×10^{-2}
219889_at	NM_005479	FRAT1	Frequently rearranged in advanced T-cell lymphomas	0.81	4.2×10^{-2}
207805_s_at	NM_002813	PSMD9	Proteasome (prosome, macropain) 26S subunit, non-ATPase, 9	0.79	4.4×10^{-2}
214080_x_at	NM_002743	PRKCSH	Protein kinase C substrate 80K-H	0.82	4.4×10^{-2}
214035_x_at	AK131084	LOC399491	LOC399491 protein	0.65	4.6×10^{-2}
205550_s_at	NM_004899	BRE	Bain and reproductive organ-expressed (TNFRSF1A modulator)	0.80	4.7×10^{-2}
212864_at	NM_003818	CDS2	CDP-diacylglycerol synthase (phosphatidate cytidyltransferase) 2	0.80	4.9×10^{-2}

* Hyperoxia/normoxia ratio of the median.

† Welch *t* test performed to determine significant genes on the filtered set of 9,787 genes.

12 (DNAJB12). This confirms previous reports of increase of HSP70 at the mRNA level in airway epithelial cells exposed to acute hyperoxia (6). There was no evidence of an increase in genes involved in the immune response or the acute-phase inflammatory response within 12 h of exposure to hyperoxia.

Cell cycle–related genes. The GOMINER functional analysis suggested a state of cell cycle arrest. The main alterations of molecular function identified were the protein phosphatases, especially with tyrosine phosphatase activity—for example, dual specificity phosphatase 7 (DUSP7), protein tyrosine phosphatase, nonreceptor type 13 (PTPN13), cell division cycle 14 homolog A (CDC14A), and tensin-like SH2 domain-containing 1 (TENS1) (Table 4, Figure 3). This was reinforced by the identification of genes involved in phosphorus metabolism, especially protein dephosphorylation and the regulation of DNA replication, that is, the significant decrease in cyclin-dependent kinase 2 (CDK2), which is involved in the late phase of G1-S transition. These findings suggest that cell cycle arrest may be an adaptive early response to cellular stress.

In Vitro Hyperoxia

Increased ubiquitination of proteins in BET-1A cells. To confirm the involvement of ubiquitin-dependent protein catabolism induced by hyperoxia at the RNA level, transformed airway epithelial BET-1A cells were exposed to hyperoxia *in vitro*. We used proteasome inhibitor ALLN at 50 μM to quantitate the total level of ubiquitination occurring over time. At this concentration there is no evidence of cell toxicity, as reported by other studies using ALLN (31, 32). Here, cells displayed a low level of ubiquitinated proteins at baseline, which increased rapidly in a time-dependent manner in response to hyperoxia exposure compared with room air exposure (Figure 4).

Increased expression of HSP 70 mRNA in BET-1A cells and HAEC. Previous study showed that upregulation of HSP70 specifically protected a lung epithelial cell line against hyperoxia by attenuating hyperoxia-mediated lipid peroxidation and ATP depletion (33). Here, primary and transformed airway epithelial cells exposed to hyperoxia *in vitro* confirmed upregulation of HSP70 mRNA by Northern analysis by 24 h of exposure (Figure 5).

Adverse effects of proteasome inhibition on ATP levels and activation/cleavage of caspase 8. To investigate the role of increased protein catabolism in cells acutely exposed to hyperoxia, airway epithelial cells were exposed to hyperoxia in the presence or absence of ALLN. No evidence of cell toxicity was observed with ALLN, which is consistent with previous studies using human airway epithelial cells (data not shown) (31, 32, 34). Total protein concentrations of cell lysates were similar in cells without ALLN and exposed to ALLN in the presence or absence of

TABLE 3. GENES UP-REGULATED IN AIRWAY EPITHELIUM WITH HYPEROXIA *IN VIVO*

Affymetrix ID	Accession No.	Symbol	Gene	Ratio*	*P* Value†
219933_at	NM_016066	GLRX2	Glutaredoxin 2	1.57	1.8×10^{-3}
201177_s_at	NM_005499	UBA2	SUMO-1 activating enzyme subunit 2	1.34	5.8×10^{-3}
206020_at	NM_004232	SOCS6	Suppressor of cytokine signaling 6	1.36	6.1×10^{-3}
219767_s_at	NM_005111	CRYZL1	Crystalline, zeta (quinone reductase)-like 1	1.26	8.0×10^{-3}
213000_at	NM_015358	ZCWCC3	Zinc finger, CW-type with coiled-coil domain 3	1.53	8.1×10^{-3}
205288_at	NM_003672	CDC14A	CDC14 cell division cycle 14 homolog A (S. cerevisiae)	1.78	8.6×10^{-3}
201801_s_at	NM_004955	SLC29A1	Solute carrier family 29 (nucleoside transporters), member 1	1.31	8.9×10^{-3}
200608_s_at	NM_006265	RAD21	RAD21 homolog (S. pombe)	1.29	9.3×10^{-3}
209146_at	NM_006745	SC4MOL	Sterol-C4-methyl oxidase-like	1.22	9.9×10^{-3}
211746_x_at	NM_148976	PSMA1	Proteasome (prosome, macropain) subunit, alpha type, 1	1.41	1.0×10^{-2}
213375_s_at	NM_052818	CG018	Hypothetical gene CG018	1.46	1.1×10^{-2}
204449_at	NM_005388	PDCL	Phosducin-like	1.59	1.1×10^{-2}
203827_at	NM_017983	FLJ10055	Hypothetical protein FLJ10055	1.37	1.1×10^{-2}
212388_at	XM_371254	USP24	Ubiquitin specific protease 24	1.41	1.1×10^{-2}
212510_at	NM_015141	KIAA0089	KIAA0089 protein	1.36	1.3×10^{-2}
203855_at	NM_014969	KIAA0893	KIAA0893 protein	1.21	1.4×10^{-2}
201816_s_at	NM_001483	GBAS	Glioblastoma amplified sequence	1.29	1.5×10^{-2}
221182_at	NM_025063	FLJ23550	Hypothetical protein FLJ23550	1.29	1.5×10^{-2}
212929_s_at	NM_001005751	LOC387680, FLJ10824	Similar to KIAA0592 protein hypothetical protein FLJ10824	1.30	1.6×10^{-2}
201803_at	NM_000938	POLR2B	Polymerase (28) II (DNA directed) polypeptide B, 140 kD	1.16	1.7×10^{-2}
209448_at	NM_006410	HTATIP2	HIV-1 Tat interactive protein 2, 30 kD	1.17	1.8×10^{-2}
211953_s_at	NM_002271	KPNB3	Karyopherin (importin) β 3	1.49	1.9×10^{-2}
208678_at	NM_001696	ATP6V1E1	ATPase, H+ transporting, lysosomal 31 kD, V1 subunit E isoform 1	1.32	2.0×10^{-2}
217851_s_at	NM_016045	C20orf45	Chromosome 20 open reading frame 45	1.46	2.1×10^{-2}
208788_at	NM_021814	ELOVL5	ELOVL family member 5, elongation of long chain fatty acids (FEN1/Elo2, SUR4/Elo3-like, yeast)	1.25	2.1×10^{-2}
201784_s_at	NM_014267	SMAP	Small acidic protein	1.49	2.2×10^{-2}
65493_at	NM_022070	ABC1	Amplified in breast cancer 1	1.44	2.2×10^{-2}
200775_s_at	NM_002140	HNRPK	Heterogeneous nuclear ribonucleoprotein K	1.56	2.3×10^{-2}
213530_at	BC022977	RAB3GAP	RAB3 GTPase-activating protein	1.16	2.4×10^{-2}
213246_at	XM_058628	C14orf109	Chromosome 14 open reading frame 109	1.36	2.4×10^{-2}
217853_at	NM_022748	TENS1	Tensin-like SH2 domain containing 1	1.44	2.4×10^{-2}
208848_at	NM_000671	ADH5	Alcohol dehydrogenase 5 (class III), chi polypeptide	1.69	2.4×10^{-2}
208638_at	NM_005742	TXNDC7	Thioredoxin domain containing 7 (protein disulfide isomerase)	1.31	2.4×10^{-2}
212819_at	NM_016114	ASB1	Ankyrin repeat and SOCS box-containing 1	1.62	2.4×10^{-2}
215884_s_at	NM_013444	UBQLN2	Ubiquilin 2	1.43	2.5×10^{-2}
212543_at	XM_166300	AIM1	Absent in melanoma 1	1.14	2.5×10^{-2}
208736_at	NM_005719	ARPC3	Actin related protein 2/3 complex, subunit 3, 21kDa	1.18	2.7×10^{-2}
204201_s_at	NM_006264	PTPN13	Protein tyrosine phosphatase, non-receptor type 13 (APO-1/CD95 (Fas)-associated phosphatase)	1.26	2.7×10^{-2}
207483_s_at	NM_018448	TIP120A	TBP-interacting protein	1.25	2.7×10^{-2}
208857_s_at	NM_005389	PCMT1	Protein-L-isoaspartate (D-aspartate) O-methyltransferase	1.32	2.7×10^{-2}
219800_s_at	NM_024838	THNSL1	Threonine synthase-like 1 (bacterial)	1.78	2.8×10^{-2}
212519_at	NM_003341	UBE2E1	Ubiquitin-conjugating enzyme E2E 1 (UBC4/5 homolog, yeast)	1.29	2.8×10^{-2}
220495_s_at	NM_024715	C5orf14	Chromosome 5 open reading frame 14	1.36	2.8×10^{-2}
209043_at	NM_005443	PAPSS1	3′-phosphoadenosine 5′-phosphosulfate synthase 1	1.22	2.9×10^{-2}
211936_at	NM_005347	HSPA5	Heat shock 70-kD protein 5 (glucose-regulated protein, 78 kD)	1.44	2.9×10^{-2}
218333_at	NM_016041	F-LANa	Carcinoma-related gene	1.50	2.9×10^{-2}
217737_x_at	NM_016407	C20orf43	Chromosome 20 open reading frame 43	1.16	2.9×10^{-2}
202872_at	NM_001695	ATP6V1C1	ATPase, H+ transporting, lysosomal 42kDa, V1 subunit C, isoform 1	1.48	3.0×10^{-2}
213848_at	NM_001947	DUSP7	Dual specificity phosphatase 7	1.30	3.0×10^{-2}
202271_at	NM_015176	KIAA0483	KIAA0483 protein	1.35	3.0×10^{-2}
212698_s_at	NM_144710	SEPT10	Septin 10	1.25	3.1×10^{-2}
201676_x_at	NM_148976	PSMA1	Proteasome (prosome, macropain) subunit, alpha type, 1	1.17	3.1×10^{-2}
206262_at	NM_000669	ADH1C	Alcohol dehydrogenase 1C (class I), gamma polypeptide	1.74	3.1×10^{-2}
203181_x_at	NM_182691	SRPK2	SFRS protein kinase 2	1.60	3.1×10^{-2}
211760_s_at	NM_003762	VAMP4	Vesicle-associated membrane protein 4	1.21	3.2×10^{-2}
200979_at	NM_000284	PDHA1	Pyruvate dehydrogenase (lipoamide) alpha 1	1.26	3.2×10^{-2}
201443_s_at	NM_005765	ATP6AP2	ATPase, H+ transporting, lysosomal accessory protein 2	1.30	3.2×10^{-2}
209273_s_at	NM_030940	HBLD2	HESB like domain containing 2	1.33	3.3×10^{-2}
212936_at	NM_032042	DKFZP564D172	Hypothetical protein DKFZp564D172	1.41	3.3×10^{-2}
212841_s_at	BC021714	PPFIBP2	PTPRF interacting protein, binding protein 2 (liprin beta 2)	1.39	3.5×10^{-2}
222016_s_at	NM_145909	ZNF323	Zinc finger protein 323	1.82	3.5×10^{-2}
211744_s_at	NM_001779	CD58	CD58 antigen, (lymphocyte function-associated antigen 3)	1.46	3.6×10^{-2}
201021_s_at	NM_006870	DSTN	Destrin (actin depolymerizing factor)	1.54	3.6×10^{-2}
210968_s_at	NM_020532	RTN4	Reticulon 4	1.19	3.7×10^{-2}
209174_s_at	NM_017730	FLJ20259	FLJ20259 protein	1.35	3.7×10^{-2}
202868_s_at	NM_006627	POP4	Processing of precursor 4, RNase P/MRP subunit (S. cerevisiae)	1.21	3.7×10^{-2}
201592_at	NM_003756	EIF3S3	Eukaryotic translation initiation factor 3, subunit 3 gamma, 40kDa	1.24	3.7×10^{-2}
211971_s_at	NM_133259	LRPPRC	Leucine-rich PPR-motif containing	1.24	3.8×10^{-2}
203773_x_at	NM_000712	BLVRA	Biliverdin reductase A	1.49	3.8×10^{-2}

(*Continued*)

TABLE 3. (*Continued*)

Affymetrix ID	Accession No.	Symbol	Gene	Ratio*	*P* Value†
203218_at	NM_002752	MAPK9	Mitogen-activated protein kinase 9	1.47	3.8×10^{-2}
209004_s_at	NM_012161	FBXL5	F-box and leucine-rich repeat protein 5	1.18	3.8×10^{-2}
202049_s_at	NM_005095	ZNF262	Zinc finger protein 262	1.29	3.8×10^{-2}
213940_s_at	NM_015033	FNBP1	Formin binding protein 1	1.47	3.9×10^{-2}
200992_at	NM_006391	IPO7	Importin 7	1.28	3.9×10^{-2}
215440_s_at	XM_043653	BEXL1	Brain expressed X-linked-like 1	1.41	3.9×10^{-2}
202474_s_at	NM_005334	HCFC1	Host cell factor C1 (VP16-accessory protein)	1.27	4.0×10^{-2}
221637_s_at	NM_024099	MGC2477	Hypothetical protein MGC2477	1.34	4.0×10^{-2}
200684_s_at	NM_003347	UBE2L3	Ubiquitin-conjugating enzyme E2L 3	1.38	4.1×10^{-2}
219751_at	NM_024860	FLJ21148	Hypothetical protein FLJ21148	1.39	4.1×10^{-2}
202854_at	NM_000194	HPRT1	Hypoxanthine phosphoribosyltransferase 1 (Lesch-Nyhan syndrome)	1.30	4.1×10^{-2}
209340_at	NM_003115	UAP1	UDP-N-acteylglucosamine pyrophosphorylase 1	1.26	4.2×10^{-2}
209034_at	NM_006813	PNRC1	Proline-rich nuclear receptor coactivator 1	1.94	4.2×10^{-2}
200780_x_at	NM_000516	GNAS	GNAS complex locus	1.31	4.3×10^{-2}
200941_at	NM_001537	HSBP1	Heat shock factor binding protein 1	1.09	4.3×10^{-2}
212956_at	XM_093895	KIAA0882	KIAA0882 protein	1.27	4.3×10^{-2}
201200_at	NM_003851	CREG	Cellular repressor of E1A-stimulated genes	1.44	4.4×10^{-2}
218065_s_at	NM_020644	C11orf15	Chromosome 11 open reading frame 15	1.19	4.6×10^{-2}
202865_at	NM_001002762	DNAJB12	DnaJ (HSP40) homolog, subfamily B, member 12	1.27	4.6×10^{-2}
202193_at	NM_005569	LIMK2	LIM domain kinase 2	1.24	4.6×10^{-2}
217731_s_at	NM_021999	ITM2B	Integral membrane protein 2B	1.74	4.6×10^{-2}
206158_s_at	NM_003418	ZNF9	Zinc finger protein 9	1.27	4.7×10^{-2}
209005_at	NM_012161	FBXL5	F-box and leucine-rich repeat protein 5	1.36	4.7×10^{-2}
209063_x_at	NM_006451	PAIP1	Poly(A) binding protein interacting protein 1	1.17	4.8×10^{-2}
212017_at	AL137406	LOC130074	Hypothetical protein LOC130074	1.20	5.0×10^{-2}
201202_at	NM_002592	PCNA	Proliferating cell nuclear antigen	1.33	5.0×10^{-2}

* Hyperoxia/normoxia ratio of the median.

† Welch *t* test performed to determine significant genes on the filtered set of 9,787 genes.

hyperoxia (all $P > 0.7$). To determine the functional consequence of blocking the proteasome pathway in terms of cell metabolism and cell death pathways, intracellular free ATP level was measured (35). Under hyperoxia, BET-1A cells increased intracellular ATP, which was consistent with the findings from the transcriptome analyses of human airway epithelium exposed to hyperoxia *in vivo* that identified upregulation of ATP synthesis as a significant biological pathway. However, the ALLN-pretreated cells exposed to hyperoxia were unable to increase the intracellular ATP level (Figure 6A). Since increased ATP is likely necessary to adjust cellular metabolism and homeostasis in stressed cells, the consequence in terms of cell death was evaluated by using caspase 8 cleavage as a marker of activation of cell death. Cleavage of caspase 8 was increased at 24 h and 48 h in hyperoxia-exposed BET-1A cells pretreated with ALLN, but not cells undergoing hyperoxia exposure only (Figure 6B). These results indicate that proteasome clearance of oxidant-damaged proteins is required for induction of energy production by the cell.

DISCUSSION

Using gene expression profiling, we identified the early integrated response of the human bronchial epithelium after hyperoxia exposure *in vivo*. This situation frequently occurs during the treatment of acute respiratory distress syndrome in the adult and the newborn, and represents an example of oxidative stress, which is a common final pathway involved in the pathogenesis of many airway diseases such as asthma, chronic obstructive pulmonary disease, and cystic fibrosis (4). Although the source of the oxidative stress differs among environmental exposure in which the oxidants are present in the inhaled air (e.g., hyperoxia, air pollution, cigarette smoke) and inflammatory airway diseases in which the inflammatory cells recruited to the airways produce ROS, the airway response to oxidants appears generally similar (1). Consistent with two genomic studies of human airway cells after oxidant stress induced by cigarette smoke *in vivo,* hyperoxia leads to a greater number of genes up-regulated than down-regulated (36, 37). This is in contrast to results from genomic analyses of whole lungs of mice exposed to hyperoxia using a similar approach to this study (38). This may be related to differences between human and murine gene responses, the use of whole murine lung tissue as opposed to our relatively pure bronchial epithelial cells obtained by brushing, or the use of different manufacturers' microarrays (36–38). Nevertheless, the fold change of responses in this study, that is, hyperoxia to normoxia ratio, for modulated genes was relatively low. One explanation may be the abundant protective levels of antioxidant scavenging molecules, including glutathione, in the extracellular epithelial lining fluid *in vivo*. This first barrier may attenuate the cellular epithelial oxidant stress in the first 12 h of hyperoxia exposure (1, 39).

Traditionally, complementary approaches were used to confirm individual genes identified in the gene expression analysis. Since the development of this powerful technology, the procedures for DNA microarrays have been carefully standardized from the design of the study to the extraction and treatment of the data to guarantee optimal confidence in the results (www.mged.org/Workgroups/MIAME/miame.html) (21, 22, 40). Recent studies validated changes in modulated genes similar in direction and magnitude when compared with semiquantitative RT-PCR (38, 41, 42). The new strategies developed to improve the validity of the analysis focus on the identification of sets of genes instead of individual genes by themselves (43, 44). In this study, we used the same approach, assuming that a set of genes displaying coordinated expression level is involved in a functional pathway. This approach is particularly well suited toward understanding the inherent complexity of biological systems; that is, the concept of systems biology is founded on models translating the results of global functional genomics into a comprehensive understanding of how organisms are organized and operate (45).

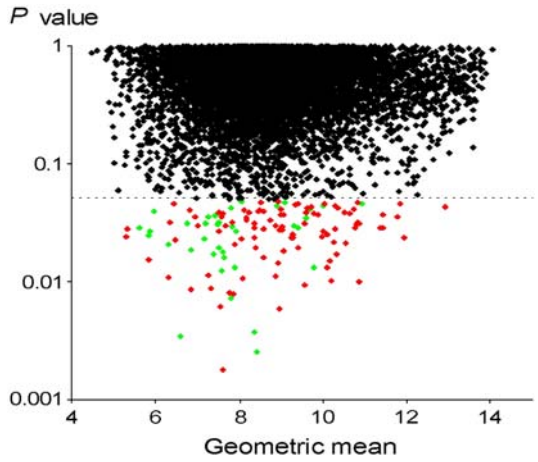

Figure 1. Genes significantly different under conditions of hyperoxia versus normoxia in five patients for expression of 9,787 genes evaluated in bronchial epithelial cells. The *P* values were calculated for each gene called "Present" and found in at least three of the four microarrays in each condition using the Welch *t* test. Ordinate, *P* value for each gene; abscissa, geometric mean of values in normoxia and hyperoxia, that is, $0.5 \times (\log_2\text{Nor} + \log_2\text{Hyp})$ (68). Genes significantly overexpressed in hyperoxia are in *red,* and significantly underexpressed in hyperoxia in *green*.

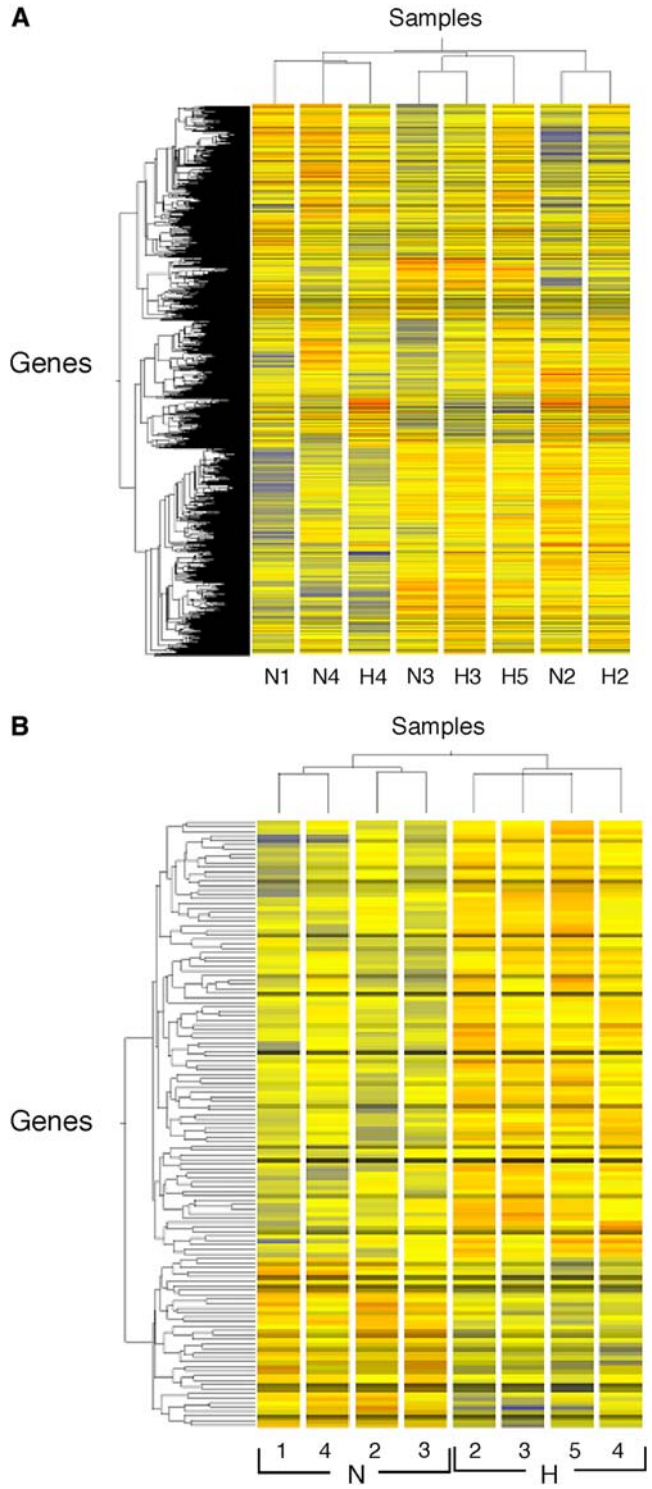

Figure 2. Hierarchical clustering of all 9,787 genes (*A*), or the subset of 135 genes differentially expressed according to a *P* value below 0.05 between hyperoxia and normoxia (*B*). Gene and condition trees were generated by hierarchical clustering of genes called "Present" in at least three of the four microarrays using the Pearson correlation. N refers to normoxia, H to hyperoxia, with numbers identifying volunteers. Using all genes (*A*), clustering occurs by pairs; for example, N3 and H3 are paired normoxia and hyperoxia of Volunteer no. 3. Using the subset of genes (*B*), clustering is by normoxia and hyperoxia groups. Individuals N1 and H5 are unpaired conditions of normoxia and hyperoxia, respectively.

Here, the inability of the bronchial epithelium to upregulate antioxidant enzymes including SOD1, SOD2, and catalase, is in accordance with previous studies showing a relatively low level of antioxidant mRNAs at baseline without any increase after 24–48 h of hyperoxia exposure in humans (7, 12, 15). The antioxidant enzyme response is similar to that of humans in murine lungs but different than in the rat (38, 46, 47). Interestingly, transgenic models with overexpression or mice deficient in these enzymes do not show evidence of an essential role of SOD and catalase in preventing hyperoxia injury in murine lungs (46). One of the protective antioxidant systems in the airway is glutathione, which neutralizes oxidants and inhibits oxidant-induced intracellular signal transduction, thus attenuating proinflammatory cellular responses (4). Human airway epithelial cell lines, including 16-HBE, BEAS-2B, NCI-H292, and A549, increase intracellular glutathione within hours of hyperoxia exposure *in vitro* (15, 48, 49). The mechanism for the glutathione increase may be related in part to a rapid, but transient, increase of glutamylcysteine ligase, the rate-limiting enzyme in *de novo* synthesis of GSH; intracellular levels increase 4 h after hyperoxia *in vitro* and return to basal levels by 12 h (50). In this study, changes in glutamylcysteine ligase mRNA were not found, but the airways were sampled after 12 h of hyperoxia, and earlier time of induction would not have been detected. However, other interacting components of the glutathione-antioxidant system, including γ-glutamyltransferase, glutathione peroxidases, and glutathione reductase, were not induced in this study, or in previous *in vitro* studies of primary human bronchial epithelial cells and bronchial epithelial cell lines exposed to hyperoxia (15, 24, 49–51). Other data support that upregulation of glutathione antioxidant systems are not requisite for defense against hyperoxia (25, 38, 52, 53). For example, glutathione peroxidase 1–deficient mice do not have increased sensitivity to hyperoxia (52, 53). Moreover, depletion of glutathione does not increase the sensitivity of BEAS-2B cells to hyperoxia (15). Taken together, enzymes of the glutathione antioxidant system do not appear to be one of the essential

TABLE 4. GOMINER CATEGORIES OF GENES MODULATED BY HYPEROXIA IN HUMAN AIRWAY EPITHELIUM *IN VIVO*

	Total*	Under*	Over*	*P* Value
Molecular Function				
Catalytic activity				
Nucleotidyl transferase activity	63	1	4	4×10^{-3}
Protein tyrosine phosphatase activity	39	0	4	4×10^{-3}
Protein tyrosine/serine/threonine phosphatase activity	20	0	2	4.2×10^{-2}
Ubiquitin conjugating enzyme activity	18	0	2	3.5×10^{-2}
Oxidoreductase activity				
Acting on aldehyde oroxo group of donors	19	1	1	4×10^{-2}
Formaldehyde dehydrogenase (glutathione) activity	1	0	1	1.6×10^{-2}
Alcohol dehydrogenase activity	6	0	2	4×10^{-3}
Transcription cofactor activity	134	2	4	2.3×10^{-2}
Corepressor activity	46	1	2	4×10^{-2}
Small GTPase binding	18	0	2	3.5×10^{-2}
Ran GTPase binding	4	0	2	2×10^{-3}
Unknown	235	2	7	1.5×10^{-2}
Biological Process				
Regulation of DNA replication	8	1	1	7×10^{-3}
Proteolysis during cellular protein catabolism	93	1	4	1.8×10^{-2}
Ubiquitin-dependent protein catabolism	81	1	4	1×10^{-2}
Protein import into nucleus, docking	13	0	2	1.9×10^{-2}
Protein modification	679	5	13	2.6×10^{-2}
Phosphorus metabolism	370	3	8	3.9×10^{-2}
Protein amino acid dephosphorylation	67	0	4	2.4×10^{-2}

* Number of genes modulated by hyperoxia and number of genes in each category on U133 array. Over- or under-representation of functional categories according to the GO classification are determined by using Fisher's exact test. Categories containing more than two genes and a *P* value < 0.05 are represented.

early adaptive responses to *in vivo* hyperoxia at the transcriptional level.

Functional analyses suggest an early effect of hyperoxia is the inhibition of DNA replication and transcription together with increased phosphatases, which would lead to a decrease in the phosphorylation status of the cell, and a possible resultant protective growth arrest. This is consistent with previous studies in mammalian and human cells exposed to hyperoxia that show

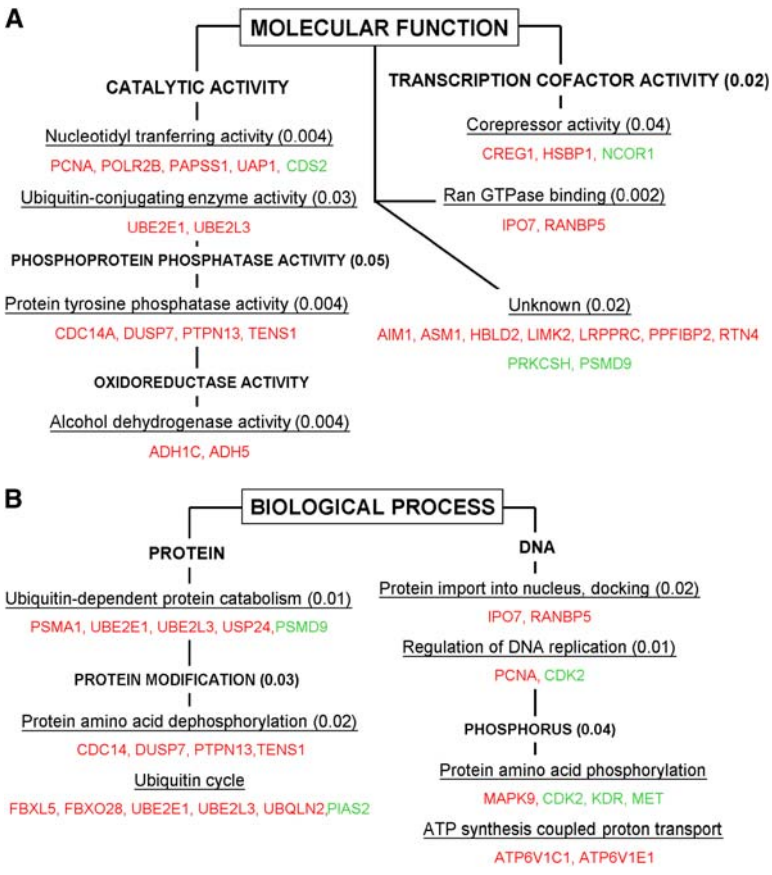

Figure 3. Selected cellular pathways triggered by hyperoxia according to the significant biological processes (*A*) and the molecular functions (*B*) involved using the GOMINER approach. Upregulated genes are represented in *red* and downregulated genes in *green*. *P* value of functional categories, using Fisher's exact test, are presented in *parentheses*. *See* tables for gene descriptions.

TABLE 5. MODULATION OF GENES INVOLVED IN REDOX REGULATION

Category	Description	Hyp/Nor ratio	*P* Value
Catalase and superoxide dismutase	Catalase	1.27	0.084
	Superoxide dismutase 1	1.05	0.683
	Superoxide dismutase 2	1.38	0.687
Glutathione metabolism	Glutathione peroxidase 1	1.51	0.35
	Glutathione peroxidase 4	1.12	0.613
	Glutathione peroxidase 2	0.92	0.798
	Glutathione peroxidase 3	1.03	0.74
	Glutathione-S-transferase A1	1.05	0.614
	Glutathione-S-transferase A2	1.30	0.298
	Glutathione-S-transferase A3	0.94	0.865
	Glutathione-S-transferase A4	1.17	0.502
	Glutathione-S-transferase M1	0.84	0.481
	Glutathione-S-transferase M2	0.94	0.808
	Glutathione-S-transferase M3	0.80	0.564
	Glutathione-S-transferase M4	0.73	0.122
	Glutathione-S-transferase M5	0.75	0.125
	Glutathione-S-transferase pi	0.98	0.963
	Glutathione-S-transferase subunit 13	1.09	0.636
	Glutathione-S-transferase theta 1	0.98	0.952
	Microsomal glutathione S-transferase 2	0.97	0.923
	Glutathione-S-transferase omega 1	1.38	0.389
	Glutathione synthetase	1	0.99
	Glutamate cysteine ligase (catalytic subunit)	1.11	0.328
	Glutamate cysteine ligase (modifier subunit)	1.17	0.217
	Glutaredoxin 2	**1.57**	**0.002**
	Glutaredoxin (thioltransferase)	1.38	0.118
Redox balance	Ferredoxin 1	1.28	0.252
	Ferredoxin reductase	1.11	0.656
	Peroxiredoxin 1	1.05	0.587
	Peroxiredoxin 2	1.00	1
	Peroxiredoxin 3	1.18	0.079
	Peroxiredoxin 4	1.34	0.396
	Peroxiredoxin 6	1.18	0.181
	Thioredoxin	1.24	0.387
	Thioredoxin 2	1.11	0.697
	Thioredoxin interacting protein	1.11	0.366
	Thioredoxin reductase 1	1.06	0.691
	Thioredoxin reductase 3	0.87	0.361
	Thioredoxin like, 32kDa	1.15	0.274
	Thioredoxin-like 2	0.98	0.839
	Thioredoxin domain containing	1.16	0.478
	Thioredoxin domain containing 4	1.04	0.681
	Thioredoxin domain containing 5	1.04	0.864
	Thioredoxin domain containing 7	**1.31**	**0.024**
	Thioredoxin-related transmembrane protein 2	1.19	0.522
	Alcohol dehydrogenase 1C	**1.74**	**0.03**
	Alcohol dehydrogenase 5	**1.33**	**0.02**
	Alcohol dehydrogenase 1A	0.96	0.792
	Alcohol dehydrogenase 6	0.90	0.505
	Alcohol dehydrogenase 7	1.22	0.442

a block of the G1 to S phase progression in the cell cycle mediated by an increase in CDK inhibitor $p21^{WAF1/CIP1}$ within the first 12 h (8, 32, 54–57). Cell cycle arrest may provide time for repair of damage sustained under hyperoxia stress, and thus avoid the replication and propagation of potentially hazardous mutations (8, 32, 56, 57). This conjecture may be supported by the decrease in CdK2 and the increase expression of genes from the protein dephosphorylation category in our study (8, 57).

The induction of genes related to the proteasome, ubiquitin-conjugation pathways, protein folding, and chaperone functions in this study suggests a carefully integrated and coordinated response to identify hyperoxia-related damaged proteins and perhaps direct them toward the protein catabolism pathway (5, 27, 58, 59). Early induction of heat shock proteins in response to hyperoxia is a well-known adaptive mechanism in the prevention of aggregation and repair of damaged cellular macromolecules, including oxidized proteins and lipids (58). Hyperoxia increases expression of HSP70 mRNA in primary bronchial epithelial cells *in vitro* (6), and HSP70 attenuates lipid peroxidation in the human airway epithelial cell line A549 exposed to hyperoxia (33). Here, upregulation of HSP70 was detected in response to hyperoxia *in vivo* and also confirmed in BET-1A and primary human airway epithelial cells exposed *in vitro.* Another important role of this molecular chaperone is to interact with the ubiquitin system (58). Ubiquitination is the process by which a polyubiquitin chain is added onto altered proteins, which allows the proteasome to recognize, bind, and unfold the ubiquitinated proteins, and subsequently digest them into small peptides (5, 26, 58, 60). Chaperones act as protein stabilizers, preventing aggregation of misfolded proteins before the ubiquitin-proteasome–dependent degradation pathway (58). Greater ubiquitination of proteins in cells exposed to hyperoxia was confirmed *in vitro*. Disturbance in the processing and degradation of proteins are implicated in the physiopathology of many diseases,

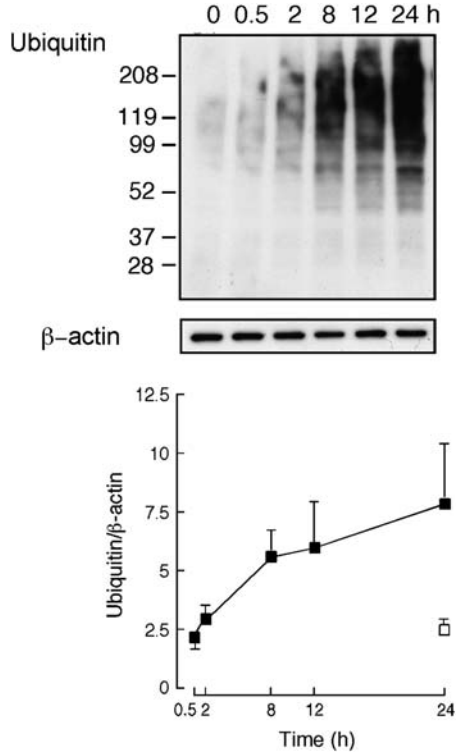

Figure 4. Ubiquitination of proteins in BET1A cells exposed to 100% O_2 increases over time. Western blot shows increase in ubiquitination of proteins over time, with β-actin as control for protein loading. Graph shows average ± SD of three independent experiments.

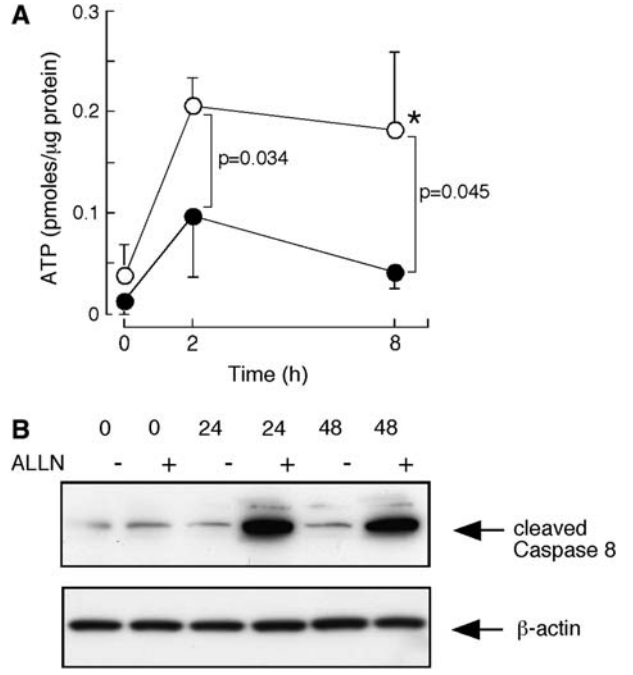

Figure 6. (*A*) ATP levels in BET1A cells exposed to 100% O_2 over time with (*closed circles*) or without (*open circles*) ALLN pretreatment. Hyperoxia induces a significant and early increase of ATP in BET1A cells without ALLN pretreatment (*$P = 0.01$). The use of ALLN prior to hyperoxia significantly reduces ATP levels within BET-1A cells. (*B*) Increased activation of cell death pathway in BET1A cells exposed to hyperoxia over time with ALLN pretreatment. Western blot shows an increase in cleaved Caspase 8 protein, with β-actin as control for protein loading. Results are representative of three independent experiments.

such as cystic fibrosis, which was recently confirmed using the same approach (32, 43, 61); hence the ability to upregulate ubiquitin-proteasome pathway is likely an essential defense to prevent tissue injury as a result of accumulation of damaged and misfolded proteins. In fact, the critical function of increasing protein clearance in hyperoxia was confirmed through measures of cellular ATP and activation of cell death pathways under conditions of inhibition of proteasomal degradation of proteins.

The ability of the cell to produce ATP in response to hyperoxia is a pivotal event in prevention of injury. An increase in glucose consumption and ATP production has previously been reported in the A549 lung cancer cell line exposed to hyperoxia (33, 62). In this study, genes involved in glycolysis were not induced *in vivo*, consistent with studies in mice exposed to hyperoxia and studies of human airway epithelial cells from individuals who smoke cigarettes (36, 38). However, hyperoxia and resultant oxidant stress may mediate effects on protein function through both transcriptional events and post-translational protein modifications. Protein tyrosine nitration, a selective and reversible process, occurs during oxidative stress, and leads to inactivation of proteins including enzymes in glycolysis and in the TCA cycle, resulting in inhibition of energy production (63). Functional genomic analysis in this study indicates that hyperoxia upregulates proteins involved in ATP production. This was confirmed by the marked and rapid induction of ATP levels in cells exposed to hyperoxia *in vitro*. The lack of increase of ATP, and the activation of caspase 8, with proteasome blockade suggests that degradation and clearance of proteins, is critical for the increase of ATP production and avoidance of cell death. Notably, the absence of apoptosis in cells exposed to hyperoxia *in vitro* was shown in previous studies of human airway epithelial cells, in which the occurrence of cell death occurs after days of exposure but appears more suggestive of necrosis (64, 65). This transcriptional signature of genes involved in ATP production (especially mitochondrial oxidoreductase activity genes) and genes involved in protein degradation (including ubiquitins) is shared among other diseases including cystic fibrosis (43) and muscular atrophy (66). These reports highlight the importance of the interaction between these pathways as a common cellular response to stress. In an *in vitro* model of human fibroblast exposure to oxidative stress, the accumulation of oxidatively modified proteins correlates with the inability of the cell to maintain intracellular ATP, with subsequent occurrence of necrosis, rather than apoptosis

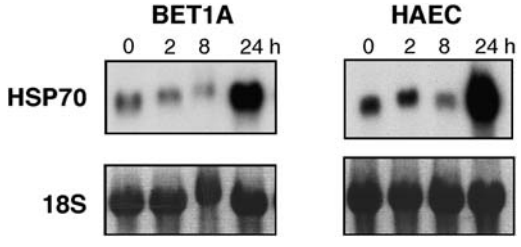

Figure 5. Time course of HSP70 mRNA expression in transformed bronchial epithelial cells (BET1A) and primary HAEC exposed to 100% O_2. The representative Northern blot analysis of total 10μg RNA/lane demonstrates an increase of HSP70 at 24 h. Ribosome 18S is shown as control. Results are representative of four independent experiments.

(67). The cell death, whether by necrosis or apoptosis, of human bronchial epithelium *in vivo* requires further studies.

In summary, human bronchial epithelial cells display small variations in gene expression after exposure to *in vivo* hyperoxia. The functional categories involved are suggestive of cell cycle arrest and induction of cytoprotective chaperones and the ubiquitin-proteasome–dependent protein degradation system. Involvement of genes with oxidoreductase activity likely contribute to maintenance of reduced glutathione and thiols that are critical for oxidant-scavenging capacity and energy production. These responses, which occur within 12 h of hyperoxia exposure *in viv*o, may be effective in preserving homeostatic integrity of the airway in the short term; however, under conditions of sustained oxygen exposure and/or chronic oxidative stress, they may not be sufficient to safeguard against injury of the airway.

***Conflict of Interest Statement*:** None of the authors has a financial relationship with a commercial entity that has an interest in the subject of this manuscript.

***Acknowledgments*:** The authors thank the Gene Expression and Genotyping Facility of the Comprehensive Cancer Center at Case (CA43703).

References

1. Comhair SA, Erzurum SC. Antioxidant responses to oxidant-mediated lung diseases. *Am J Physiol Lung Cell Mol Physiol* 2002;283:L246–L255.
2. Heffner JE, Repine JE. Pulmonary strategies of antioxidant defense. *Am Rev Respir Dis* 1989;140:531–554.
3. van der Vliet A, Cross CE. Oxidants, nitrosants, and the lung. *Am J Med* 2000;109:398–421.
4. Rahman I, MacNee W. Oxidative stress and regulation of glutathione in lung inflammation. *Eur Respir J* 2000;16:534–554.
5. Grune T, Reinheckel T, Davies KJ. Degradation of oxidized proteins in mammalian cells. *FASEB J* 1997;11:526–534.
6. Yoo JH, Erzurum SC, Hay JG, Lemarchand P, Crystal RG. Vulnerability of the human airway epithelium to hyperoxia: constitutive expression of the catalase gene in human bronchial epithelial cells despite oxidant stress. *J Clin Invest* 1994;93:297–302.
7. Comhair SA, Thomassen MJ, Erzurum SC. Differential induction of extracellular glutathione peroxidase and nitric oxide synthase 2 in airways of healthy individuals exposed to 100% O_2 or cigarette smoke. *Am J Respir Cell Mol Biol* 2000;23:350–354.
8. Barazzone C, Horowitz S, Donati YR, Rodriguez I, Piguet PF. Oxygen toxicity in mouse lung: pathways to cell death. *Am J Respir Cell Mol Biol* 1998;19:573–581.
9. Carvalho CR, de Paula Pinto Schettino G, Maranhao B, Bethlem EP. Hyperoxia and lung disease. *Curr Opin Pulm Med* 1998;4:300–304.
10. Jobe AH, Bancalari E. Bronchopulmonary dysplasia. *Am J Respir Crit Care Med* 2001;163:1723–1729.
11. Comroe J. Oxygen toxicity: the effect of inhalation of high concentration of oxygen for 24 hours on normal men at sea level and at a simulated altitude of 18,000 feet. *JAMA* 1945;128:710–717.
12. Erzurum SC, Danel C, Gillissen A, Chu CS, Trapnell BC, Crystal RG. In vivo antioxidant gene expression in human airway epithelium of normal individuals exposed to 100% O2. *J Appl Physiol* 1993;75:1256–1262.
13. Sackner MA, Landa J, Hirsch J, Zapata A. Pulmonary effects of oxygen breathing: a 6-hour study in normal men. *Ann Intern Med* 1975;82: 40–43.
14. Danel C, Erzurum SC, Prayssac P, Eissa NT, Crystal RG, Herve P, Baudet B, Mazmanian M, Lemarchand P. Gene therapy for oxidant injury-related diseases: adenovirus-mediated transfer of superoxide dismutase and catalase cDNAs protects against hyperoxia but not against ischemia-reperfusion lung injury. *Hum Gene Ther* 1998;9:1487–1496.
15. Pietarinen-Runtti P, Raivio KO, Saksela M, Asikainen TM, Kinnula VL. Antioxidant enzyme regulation and resistance to oxidants of human bronchial epithelial cells cultured under hyperoxic conditions. *Am J Respir Cell Mol Biol* 1998;19:286–292.
16. Grune T, Merker K, Sandig G, Davies KJ. Selective degradation of oxidatively modified protein substrates by the proteasome. *Biochem Biophys Res Commun* 2003;305:709–718.
17. Erzurum SC, Lemarchand P, Rosenfeld MA, Yoo JH, Crystal RG. Protection of human endothelial cells from oxidant injury by adenovirus-mediated transfer of the human catalase cDNA. *Nucleic Acids Res* 1993;21:1607–1612.
18. Lillig CH, Berndt C, Vergnolle O, Lonn ME, Hudemann C, Bill E, Holmgren A. Characterization of human glutaredoxin 2 as iron-sulfur protein: a possible role as redox sensor. *Proc Natl Acad Sci USA* 2005; 102:8168–8173.
19. Liu G, Loraine AE, Shigeta R, Cline M, Cheng J, Valmeekam V, Sun S, Kulp D, Siani-Rose MA. NetAffx: Affymetrix probesets and annotations. *Nucleic Acids Res* 2003;31:82–86.
20. Eisen MB, Spellman PT, Brown PO, Botstein D. Cluster analysis and display of genome-wide expression patterns. *Proc Natl Acad Sci USA* 1998;95:14863–14868.
21. Ashburner M, Ball CA, Blake JA, Botstein D, Butler H, Cherry JM, Davis AP, Dolinski K, Dwight SS, Eppig JT, *et al.* Gene ontology: tool for the unification of biology. The Gene Ontology Consortium. *Nat Genet* 2000;25:25–29.
22. Zeeberg BR, Feng W, Wang G, Wang MD, Fojo AT, Sunshine M, Narasimhan S, Kane DW, Reinhold WC, Lababidi S, *et al.* GoMiner: a resource for biological interpretation of genomic and proteomic data. *Genome Biol* 2003;4:R28.
23. Reddel RR, Ke Y, Gerwin BI, McMenamin MG, Lechner JF, Su RT, Brash DE, Park JB, Rhim JS, Harris CC. Transformation of human bronchial epithelial cells by infection with SV40 or adenovirus-12 SV40 hybrid virus, or transfection via strontium phosphate coprecipitation with a plasmid containing SV40 early region genes. *Cancer Res* 1988; 48:1904–1909.
24. Comhair SA, Bhathena PR, Farver C, Thunnissen FB, Erzurum SC. Extracellular glutathione peroxidase induction in asthmatic lungs: evidence for redox regulation of expression in human airway epithelial cells. *FASEB J* 2001;15:70–78.
25. Wu BJ, Morimoto RI. Transcription of the human hsp70 gene is induced by serum stimulation. *Proc Natl Acad Sci USA* 1985;82:6070–6074.
26. Donati YR, Slosman DO, Polla BS. Oxidative injury and the heat shock response. *Biochem Pharmacol* 1990;40:2571–2577.
27. Kolodziejski PJ, Musial A, Koo JS, Eissa NT. Ubiquitination of inducible nitric oxide synthase is required for its degradation. *Proc Natl Acad Sci USA* 2002;99:12315–12320.
28. Enoksson M, Fernandes AP, Prast S, Lillig CH, Holmgren A, Orrenius S. Overexpression of glutaredoxin 2 attenuates apoptosis by preventing cytochrome c release. *Biochem Biophys Res Commun* 2005;327:774–779.
29. Liu L, Hausladen A, Zeng M, Que L, Heitman J, Stamler JS. A metabolic enzyme for S-nitrosothiol conserved from bacteria to humans. *Nature* 2001;410:490–494.
30. Gaston B, Reilly J, Drazen JM, Fackler J, Ramdev P, Arnelle D, Mullins ME, Sugarbaker DJ, Chee C, Singel DJ, *et al.* Endogenous nitrogen oxides and bronchodilator S-nitrosothiols in human airways. *Proc Natl Acad Sci USA* 1993;90:10957–10961.
31. Gerber A, Heimburg A, Reisenauer A, Wille A, Welte T, Buhling F. Proteasome inhibitors modulate chemokine production in lung epithelial and monocytic cells. *Eur Respir J* 2004;24:40–48.
32. Boncoeur E, Tabary O, Bonvin E, Muselet C, Fritah A, Lefait E, Redeuilh G, Clement A, Jacquot J, Henrion-Caude A. Oxidative stress response results in increased p21(WAF1/CIP1) degradation in cystic fibrosis lung epithelial cells. *Free Radic Biol Med* 2006;40:75–86.
33. Wong HR, Menendez IY, Ryan MA, Denenberg AG, Wispe JR. Increased expression of heat shock protein-70 protects A549 cells against hyperoxia. *Am J Physiol* 1998;275:L836–L841.
34. Wu HM, Wen HC, Lin WW. Proteasome inhibitors stimulate interleukin-8 expression via Ras and apoptosis signal-regulating kinase-dependent extracellular signal-related kinase and c-Jun N-terminal kinase activation. *Am J Respir Cell Mol Biol* 2002;27:234–243.
35. Eguchi Y, Shimizu S, Tsujimoto Y. Intracellular ATP levels determine cell death fate by apoptosis or necrosis. *Cancer Res* 1997;57:1835–1840.
36. Hackett NR, Heguy A, Harvey BG, O'Connor TP, Luettich K, Flieder DB, Kaplan R, Crystal RG. Variability of antioxidant-related gene expression in the airway epithelium of cigarette smokers. *Am J Respir Cell Mol Biol* 2003;29:331–343.
37. Spira A, Beane J, Shah V, Liu G, Schembri F, Yang X, Palma J, Brody JS. Effects of cigarette smoke on the human airway epithelial cell transcriptome. *Proc Natl Acad Sci USA* 2004;101:10143–10148.
38. Perkowski S, Sun J, Singhal S, Santiago J, Leikauf GD, Albelda SM. Gene expression profiling of the early pulmonary response to hyperoxia in mice. *Am J Respir Cell Mol Biol* 2003;28:682–696.
39. Comhair SA, Lewis MJ, Bhathena PR, Hammel JP, Erzurum SC. Increased glutathione and glutathione peroxidase in lungs of individuals

with chronic beryllium disease. *Am J Respir Crit Care Med* 1999;159: 1824–1829.
40. Kaminski N, Friedman N. Practical approaches to analyzing results of microarray experiments. *Am J Respir Cell Mol Biol* 2002;27:125–132.
41. Spira A, Beane J, Pinto-Plata V, Kadar A, Liu G, Shah V, Celli B, Brody JS. Gene expression profiling of human lung tissue from smokers with severe emphysema. *Am J Respir Cell Mol Biol* 2004;31:601–610.
42. Irizarry RA, Warren D, Spencer F, Kim IF, Biswal S, Frank BC, Gabrielson E, Garcia JG, Geoghegan J, Germino G, *et al.* Multiple-laboratory comparison of microarray platforms. *Nat Methods* 2005;2: 345–350.
43. Wright JM, Merlo CA, Reynolds JB, Zeitlin PL, Garcia JGN, Guggino WB, Boyle MP. Respiratory epithelial gene expression in patients with mild and severe cystic fibrosis lung disease. *Am J Respir Cell Mol Biol* 2006;35:327–336.
44. Gruber MP, Coldren CD, Woolum MD, Cosgrove GP, Zeng C, Baron AE, Moore MD, Cool CD, Worthen GS, Brown KK, *et al*. Human lung project: evaluating variance of gene expression in the human lung. *Am J Respir Cell Mol Biol* 2006;35:65–71.
45. Strange K. The end of "naive reductionism": rise of systems biology or renaissance of physiology? *Am J Physiol Cell Physiol* 2005;288:C968–C974.
46. Waxman AB, Einarsson O, Seres T, Knickelbein RG, Warshaw JB, Johnston R, Homer RJ, Elias JA. Targeted lung expression of interleukin-11 enhances murine tolerance of 100% oxygen and diminishes hyperoxia-induced DNA fragmentation. *J Clin Invest* 1998;101:1970–1982.
47. Ho YS, Dey MS, Crapo JD. Antioxidant enzyme expression in rat lungs during hyperoxia. *Am J Physiol* 1996;270:L810–L818.
48. Rahman I, Mulier B, Gilmour PS, Watchorn T, Donaldson K, Jeffery PK, MacNee W. Oxidant-mediated lung epithelial cell tolerance: the role of intracellular glutathione and nuclear factor-kappaB. *Biochem Pharmacol* 2001;62:787–794.
49. Ray S, Watkins DN, Misso NL, Thompson PJ. Oxidant stress induces gamma-glutamylcysteine synthetase and glutathione synthesis in human bronchial epithelial NCI-H292 cells. *Clin Exp Allergy* 2002;32: 571–577.
50. Rahman I, Bel A, Mulier B, Donaldson K, MacNee W. Differential regulation of glutathione by oxidants and dexamethasone in alveolar epithelial cells. *Am J Physiol* 1998;275:L80–L86.
51. van Klaveren RJ, Demedts M, Nemery B. Cellular glutathione turnover in vitro, with emphasis on type II pneumocytes. *Eur Respir J* 1997;10: 1392–1400.
52. Cho HY, Jedlicka AE, Reddy SP, Kensler TW, Yamamoto M, Zhang LY, Kleeberger SR. Role of NRF2 in protection against hyperoxic lung injury in mice. *Am J Respir Cell Mol Biol* 2002;26:175–182.
53. Ho YS, Magnenat JL, Bronson RT, Cao J, Gargano M, Sugawara M, Funk CD. Mice deficient in cellular glutathione peroxidase develop normally and show no increased sensitivity to hyperoxia. *J Biol Chem* 1997;272:16644–16651.
54. McGrath SA. Induction of p21WAF/CIP1 during hyperoxia. *Am J Respir Cell Mol Biol* 1998;18:179–187.
55. Corroyer S, Maitre B, Cazals V, Clement A. Altered regulation of G1 cyclins in oxidant-induced growth arrest of lung alveolar epithelial cells: accumulation of inactive cyclin E-DCK2 complexes. *J Biol Chem* 1996;271:25117–25125.
56. O'Reilly MA, Staversky RJ, Watkins RH, Reed CK, de Mesy Jensen KL, Finkelstein JN, Keng PC. The cyclin-dependent kinase inhibitor p21 protects the lung from oxidative stress. *Am J Respir Cell Mol Biol* 2001;24:703–710.
57. Helt CE, Staversky RJ, Lee YJ, Bambara RA, Keng PC, O'Reilly MA. The Cdk and PCNA domains on p21Cip1 both function to inhibit G1/S progression during hyperoxia. *Am J Physiol Lung Cell Mol Physiol* 2004;286:L506–L513.
58. Goldberg AL. Protein degradation and protection against misfolded or damaged proteins. *Nature* 2003;426:895–899.
59. Horibe T, Gomi M, Iguchi D, Ito H, Kitamura Y, Masuoka T, Tsujimoto I, Kimura T, Kikuchi M. Different contributions of the three CXXC motifs of human protein-disulfide isomerase-related protein to isomerase activity and oxidative refolding. *J Biol Chem* 2004;279:4604–4611.
60. Ciechanover A. Proteolysis: from the lysosome to ubiquitin and the proteasome. *Nat Rev Mol Cell Biol* 2005;6:79–87.
61. Zeitlin PL, Gail DB, Banks-Schlegel S. Protein processing and degradation in pulmonary health and disease. *Am J Respir Cell Mol Biol* 2003; 29:642–645.
62. Allen CB, White CW. Glucose modulates cell death due to normobaric hyperoxia by maintaining cellular ATP. *Am J Physiol* 1998;274:L159–L164.
63. Aulak KS, Koeck T, Crabb JW, Stuehr DJ. Dynamics of protein nitration in cells and mitochondria. *Am J Physiol Heart Circ Physiol* 2004;286: H30–H38.
64. Kazzaz JA, Xu J, Palaia TA, Mantell L, Fein AM, Horowitz S. Cellular oxygen toxicity. Oxidant injury without apoptosis. *J Biol Chem* 1996; 271:15182–15186.
65. Mantell LL, Lee PJ. Signal transduction pathways in hyperoxia-induced lung cell death. *Mol Genet Metab* 2000;71:359–370.
66. Lecker SH, Jagoe RT, Gilbert A, Gomes M, Baracos V, Bailey J, Price SR, Mitch WE, Goldberg AL. Multiple types of skeletal muscle atrophy involve a common program of changes in gene expression. *FASEB J* 2004;18:39–51.
67. Miyoshi N, Oubrahim H, Chock PB, Stadtman ER. Age-dependent cell death and the role of ATP in hydrogen peroxide-induced apoptosis and necrosis. *Proc Natl Acad Sci USA* 2006;103:1727–1731.
68. Dudoit SD, Y. Y., Callow MJ, Speed TP. Statistical methods for identifying differently expressed genes in replicated cDNA microarray experiments. Technical Report #578. Stanford: Stanford University; 2000. p. 38.